Journal of Mines, Metals and Fuels, *71(12C) : 58-65; 2023. DOI: 10.18311/jmmf/2023/47264*

Print ISSN : 0022-2755

Journal of Mines, Metals and Fuels

Contents available at: *www.informaticsjournals.com/index.php/jmmf*

Temperature-dependent Growth Mechanism of PVP-based Copper Sulfide (CuS) Nanocomposite

H. K. Deepa*, A. Jagannatha Reddy and Kalpana Sharma

Department of Physics, M S Ramaiah Institute of Technology (Affiliated to VTU), Bengaluru – 560054, Karnataka, India; deepahk289@gmail.com

Abstract

This study focuses on the proficient synthesis of a Copper Sulfide (CuS) nanocomposite using the hydrothermal method at four distinct reaction temperatures: 130°C, 150°C, 170°C, and 200°C, each with a 5-hour duration. Comprehensive characterization through Powder X-ray Diffraction (PXRD), UV-visible spectroscopy (UV-vis), and Scanning Electron Microscopy (SEM) has been undertaken to analyze the morphological, optical, and compositional aspects of the synthesized sample. Key findings include the identification of a hexagonal phase of CuS nanostructures, closely aligned with reference data (JCPDS card no 9000062), and an average crystallite size ranging from 17nm to 26nm. SEM imaging reveals a distinctive petal-like flower morphology in the CuS nanomaterial. Energy Dispersive Spectra (EDS) confirms the presence of copper (Cu) and sulfur (S) elements in the nanocomposite. The optical analysis demonstrates a direct type of allowed transition and variable band gap values (ranging from 2.07eV to 1.92eV), suggesting potential applications in optoelectronics and the significant influence of reaction temperature on the stability and size of the CuS nanocomposite, highlighting the critical role of temperature control in the synthesis process.

Keywords: *CuS Nanoparticles, EDS, PXRD, SEM, Stabilizing Agent, UV-vis*

1.0 Introduction

In recent years, vast research interest has been developed worldwide in revising transition metal-semiconductor nanoparticles. In contrast to other nanoparticles derived from transition metals, copper-based nanomaterials are experiencing widespread popularity globally. This can be attributed to their abundant availability, cost-effectiveness, and the inherent possession of favorable optical and electrical properties[1]. Transition metal sulfides are an emerging field in research because of their attractive optical, catalytic, and electronic properties and applications[2,3]. Copper sulfides, notably chalcopyrite ($CuFeS_2$), covellite (CuS), and chalcocite (Cu_2S), represent the predominant and consequently primary mineral constituents in the global copper mining sector[4]. The study reveals that Copper Sulphide is a prime P-type semiconductor with Copper vacancies in the lattice[5]. They are extensively studied for their applications likely as optical filters, solar cells, sensors, superconductors at low temperatures below 1.6K, and cathode material in Lithium-ion batteries[6-8]. CuS nanomaterials hold significant promise for deployment as adsorption agents in the mining industry, facilitating the extraction and quantification of noble metal ions, such as Au^{3+}, Pd^{2+}, and Pt^{4+}. This is especially advantageous when faced with complex mixtures of multiple metal ions, enabling efficient separation and elution processes for standard ore samples[9]. For the fabrication of CuS nanostructures such as nanorods, nanobelts, nanowires, nanocrystals, and nanotubes, several synthesis methods have been followed, like hydrothermal and solvothermal,

*Author for correspondence

microwave irradiation, template-assisted growth[10-13], and many more. Copper sulfide exhibits distinct crystallographic phases. Its optimal band gap renders it a highly effective solar absorber, owing to its variable band gap characteristics. This variability can be precisely tailored to the ideal band gap by synthesizing copper sulfide nanostructures with diverse morphologies[14]. This engineering process involves meticulous control over parameters such as temperature, pressure, precursor concentrations, and reaction time. In comparison with other synthesis methods, the hydrothermal technique is one of the simplest and solution reaction-based approaches, where water is used as a solvent for uniform dispersion of the precursors at high temperature and pressure to synthesize tuneable nanostructured materials.

In this study, we have successfully synthesized CuS nanoparticles at four distinct reaction temperatures, namely 120°C, 150°C, 170°C, and 200°C, while maintaining a consistent reaction duration of 5 hours. Our investigation is focused on assessing the impact of reaction temperature on the structural and optical characteristics of these nanoparticles.

2.0 Experimental Sections

2.1 Experimental Materials

In this experimental synthesis, all reagents purchased were analytically pure. Copper chloride dihydrate [$Cu(Cl_2)2H_2O$] from Sigma Aldrich, Deionized water, Sodium thiosulphate pentahydrate from Merck India, and PVP(K30) were brought and utilized without any further purification.

2.2 Material Synthesis

1mmol $Cu(Cl_2)2H_2O$ was dissolved in 40ml Deionised water and the solution appeared blue. Then 3mmol [$Na_2S_2O_35H_2O$] and PVPK (30) were added to the prepared solution. The solution was stirred using a stirrer and a magnetic bead for 45 mins. The mixture was autoclaved and treated at four different reaction temperatures 130, 150, 170 and 200°C, respectively[15]. The entire mixture was left to cool to attain room temperature. Ultimately the resultant black precipitation was collected and centrifuged with water and ethanol several times to remove the impurity traces and was dried at 60°C for 5 hrs.

2.3 Characterization

X-RAY Powder Diffraction (XRD) of the products was carried out using Rigaku HR X-ray diffractometer with CuKα radiation (λ.= 1.5418A°). SEM/EDS analysis was carried out on a Scanning Electron Microscope. UV-vis absorption spectra were recorded using a UV-Visible spectrometer (Lambda 950, Perkin Elmer), utilizing deionized water as the reference solvent.

3.0 Results and Discussion

3.1 X-Ray Diffraction (XRD) Analysis

The XRD patterns of CuS nanocomposite synthesized using copper chloride as a Cu precursor, Sodium thiosulphate as a Sulphur source, and PVP as a stabilizer at four different reaction temperatures 130°C, 150°C, 170°C, and 200°C, respectively for a reaction time of 5 hrs are shown in Figure 1. The XRD pattern, reveals the formation of CuS nanostructure with covellite phase belonging to hexagonal crystal system matched with the JCPDS card no (9000062) and cell parameters, a=b=3.7960 and c=16.3600. For a hexagonal system, the cell parameters are a=b≠c and α=β=90° γ=120°. XRD pattern consists of a few other peaks which mark the traces of impurities in the sample and broader peaks also suggest that the yielded CuS nanostructure samples are of smaller crystallites. The XRD graph noticeably shows the presence of clear diffraction patterns at 2θ = 27.65, 29.25, 31.76, 32.82, 47.71, 47.89, 52.67, and 59.27 corresponding to the (101), (102), (103), (006), (110), (108) and (116) planes, respectively in agreement with the JCPDS file indicating that CuS exists as a covellite phase[16,17].

The figure shows that the peaks are intense and sharper for an extended reaction temperature. This could be due to the rate of nucleation that would increase at extended temperatures due to Ostwald ripening[18,19]. As nanostructures have limited lattice volume, the increase in particle size yields in the increase of the d-spacing within the lattice, and the growth in the particle size induces the diffraction peaks to get shifted to lower angles which results in narrow peak broadening and high-intensity peaks as observed in the above XRD pattern at elevated temperatures.

The crystallite size of CuS nanomaterials was calculated by using Scherer's formula as follows[18]

$$D = \frac{0.9\lambda}{\beta \cos\theta} \qquad \ldots\ldots\ldots\ldots\ldots (1)$$

where, D = is the size of the particle, K = is known as the Scherer's constant and is equal to (K=0.94), λ = denotes the X-RAY wavelength (1.5418 A^{O}), β = is Full-Width Half Maximum (FWHM) intensity of the peak (in Radians) and 2θ = is the angle of diffraction.

The average grain size was found to be 17, 18, 23, and 26 nm for different temperatures at 130°C, 150°C, 170°C, and 200°C, respectively. This reveals the grain growth at elevated temperatures.

Dislocation density is a measure of the number of dislocations per unit volume and is denoted by (δ)[18]

$$\delta = \frac{1}{D2} \quad \ldots\ldots (2)$$

The strain (ε) can be calculated using the relation

$$\varepsilon = \beta \div 4\tan \quad \ldots\ldots\ldots (3)$$

In Table 1, the estimated dislocation density (δ) and strain (ε) are summarized. From table, it is very precise to explain how the decreasing values of dislocation density and strain influence the crystal imperfections at elevated temperatures, with most defects removed from the lattice until it reaches a distinct stable structure. Hence it is inferred that dislocation density (δ) and strain (ε) values decrease with increase in temperatures.

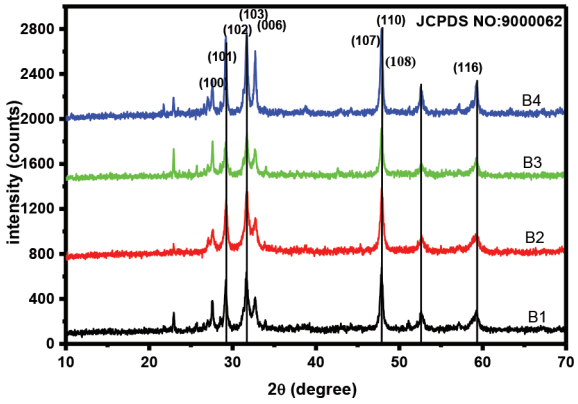


Figure 1. XRD pattern of CuS nanostructures synthesised using copper chloride, sodium thiosulphate and PVP for 5hrs at different temperatures B1) 130°C B2) 150°C B3) 170°C B4) 200°C.

3.2 UV-VIS Spectroscopic (UV-vis) Analysis

Figure 2 shows the UV-Vis absorption spectra of the successive CuS nanostructures. From the figure, it is evident that the samples absorb radiation in the spectral region between 200 to 800 nm. In the near IR region and visible region, there is a prominent absorption peak at lower temperatures. It is also observed that the broadband protrudes into the near-IR region, which confirms the characteristic of CuS covellite. The UV-Vis spectrum of as-synthesized CuS nanocomposite is slightly red-shifted at -higher temperatures, in contrast to the bulk CuS material[20,21]. In the mid-visible region, the CuS nanocomposite has a maximum absorption peak in the range between 450 to 550nm, indicating that CuS can be a favorable material in the field of solar cells and photo-catalysis.

With the help of absorption spectra, the band gap (Eg) can be obtained using the following equation[22].

$$\alpha hv^{n} = Ahv - Eg \quad (1)$$

The energy band gap can be determined by plotting (αhv)n versus (hv), where "α" is the absorption coefficient, "hv" is the energy of the photon "A" is a constant "Eg" is the band gap energy and "n" can either be ½ or 2 depending on direct transition or indirect transition[23,24]. Therefore, a plot of (αhv) versus (hv) gives a straight line and the intercept on the energy axis gives the energy gap.

The UV-Vis absorption is much broader in the visible region (400 to 550nm) and this indicates that CuS nanostructure has great potential in the field of optoelectronics[25]. Many other factors influence the

Table 1. Estimated average crystallite size, dislocation density, and strain from XRD data at different extended temperatures

Trial	Temp(°C)	2(°)	β (FWHM)(°)	Sherrer Method D(nm)$_{103\ plane}$	d-spacing (Å)	δ×10^{-3} (nm^{-2})	ε ×10^{-3}
1.	130	31.625	0.461	17nm	2.827	3.121	7.105
2.	150	31.725	0.458	18nm	2.819	3.086	7.035
3.	170	31.661	0.353	23nm	2.824	1.810	5.434
4.	200	31.659	0.310	26nm	2.824	1.413	4.772

electronic transition within the nanostructures, likely the presence of surface defects, such as oxygen vacancies, interstitials, structural disorders, and even excitonic transitions[26-28]. The graph also shows that the absorption peak is maximum and broad for elevated temperatures.

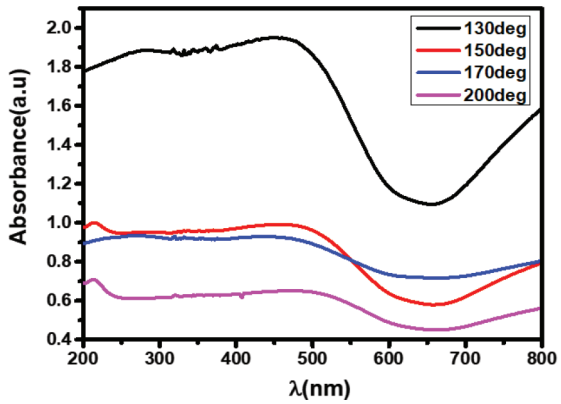
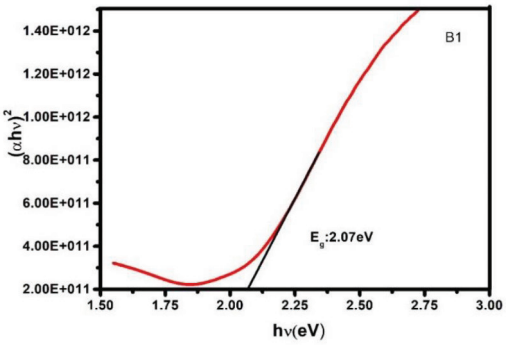
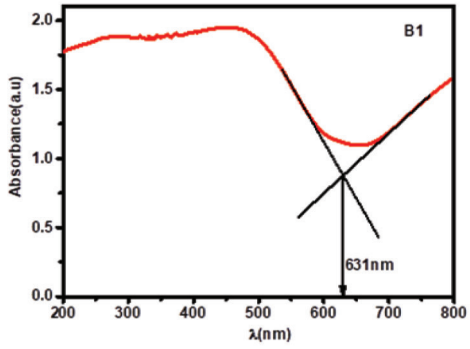


Figure 2. UV-VIS absorption spectra of CuS samples synthesized at different temperatures of B1) 130°C, B2) 150°C, B3) 170°C and B4) 200°C.



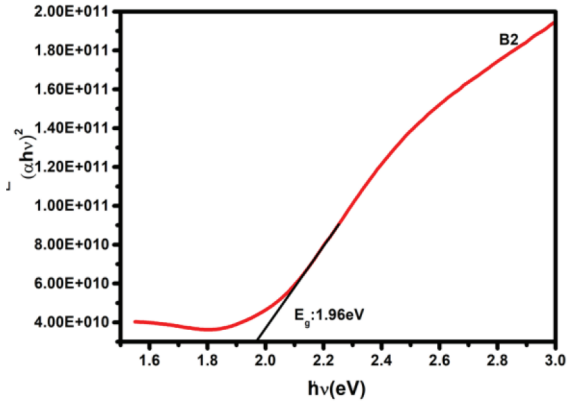
Tauc plot B1



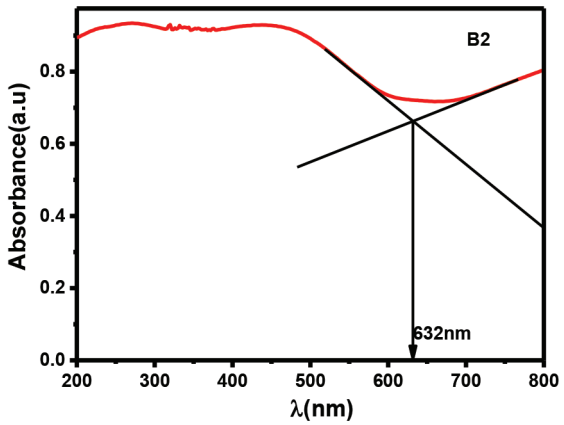
Absorption Edge B1

Figure 3. Bandgap plot using Tauc Plot and Absorption Edge (λ) at different temperatures of B1) 130°C, B2) 150°C, B3) 170°C and B4) 200°C.

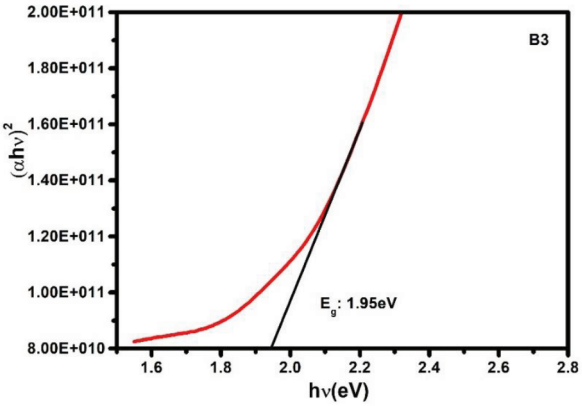
This reveals that the particle size increases with an increase in wavelength. These verdicts confirm that the as-synthesized CuS nanocomposite is a potential material in solar cells and photocatalysis.



Tauc Plot B2



Absorption Edge B2

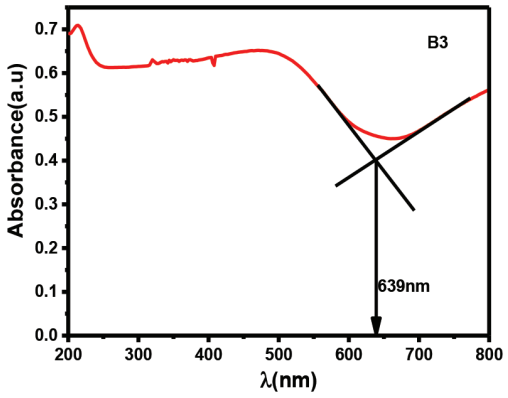


Tauc Plot B3

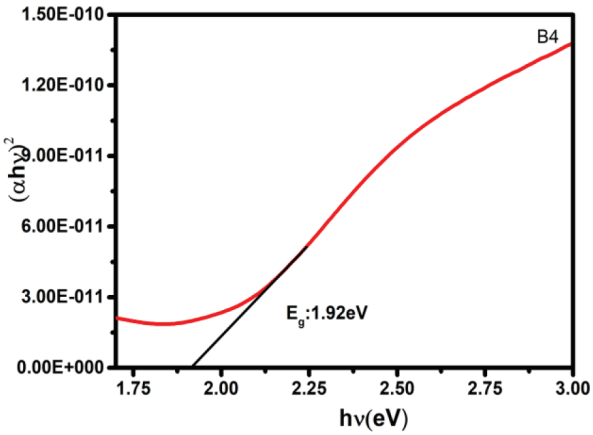
Figure 3. Continued...

The λ_{max} and absorption edge of the as synthesised nanocomoposites at four different temperatures is tabulated in the Table 2 as shown in Figure 3.

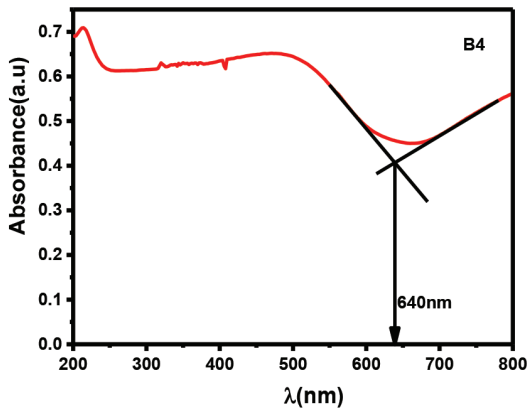
From the nature of the taut plot, it is evident that the allowed transition is direct. In the direct transition both energy and momentum are conserved and the relation of the absorption coefficient(α) to the energy of the photon depends on the type of transition[29,30]. Based on direct transition and equating in eq (1), the band gaps obtained for CuS nanocomposites are tabulated in Table 2: 2.07 eV, 1.96 eV, 1.95eV, and 1.92 eV for four different temperatures of 130, 150, 170, and 200°C, respectively. The λ_{max} of the as-synthesized nanocomposite is tabulated and is shown in the Table 2.



Absorption Edge B3



Tauc Plot B4



Absorption Edge B4

Figure 3. Continued...

3.3 Scanning Electron Microscopy (SEM) Analysis

Based on the SEM images shown in Figure 4, the morphology of the sample revealed that the samples of CuS appeared irregular flower-like nanostructures of uniform distribution. Also, the elemental composition of CuS nanostructures was confirmed using Energy Dispersive Spectroscopy [EDS]. Different temperatures can influence the growth kinetics of various crystal

Table 2. Estimation of Bandgap using TAUC Plot and Absorption Edge(λ) at different temperatures B1) 130°C, B2) 150°C, B3) 170°C and B4) 200°C

Trial	Temp(°C)	Absorption edge (λ_{edge})	Band gap $E_{g(Tauc\ plot)}$	Band gap E_g=1240/ λ_{edge}
B1.	**130°C**	631nm	2.07eV	1.97Ev
B2.	**150°C**	632nm	1.96eV	1.96eV
B3.	**170°C**	639nm	1.95eV	1.94Ev
B4.	**200°C**	640nm	1.92eV	1.93Ev

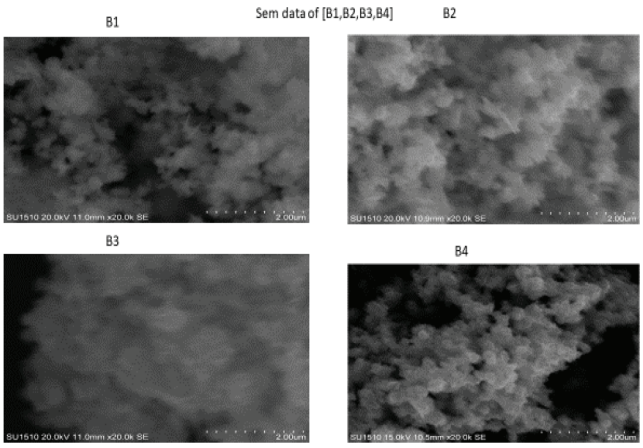


Figure 4. SEM images of CuS nanostructures for 5 hrs at different temperatures B1) 130°C, B2) 150°C, B3) 170°C and B4) 200°C.

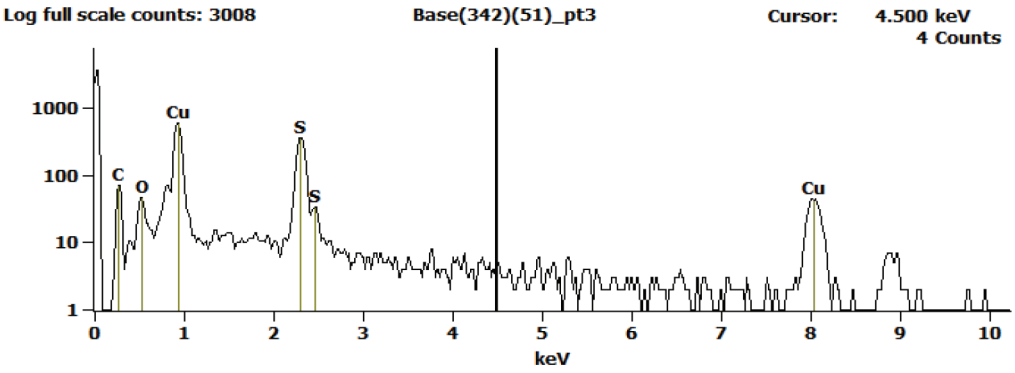


Figure 5. EDX/EDS spectra. B1) 130°C, B2) 150°C, B3) 170°C and B4) 200°C.

facets, forming specific shapes such as spheres, needles, and petals like as shown in the SEM image. The observation results revealed that temperature plays a vital role in the morphology and crystallinity of the resultant samples. From the SEM images it is evident that, at elevated temperatures, the grain size of the CuS nanostructures formed appears to be denser and more crystallized. This could be due to the hydrolysis rates of copper n sulfur precursors in water in the formation of CuS nanostructures at different temperatures under hydrothermal conditions.

As the reaction temperature increases, the morphologies of as-obtained CuS become distinct having petal-like flower morphology, as shown in SEM images. The formation of any nanostructures usually involves nucleation. Nucleation in the case of CuS nanocomposite, it is observed that the initial nucleating stage consists of needle-like seeds and eventually they grow along different planes which induces the growth process[31]. Meanwhile, the surfactant added to the precursors in the synthesis of CuS prevents the seeds' aggregation, and the reaction temperature and time promote the arrangement of the needle-like structures into petal-like nanoflower to form the self-assembled nanostructures.

3.4 Energy-dispersive X-ray Spectroscopy (EDX / EDS) Analysis

From the EDX/EDS spectra shown in the Figure 5, it can be seen that the surface of the particles appears to be undefined. The EDS patterns show copper and sulfur confirming the formation of CuS nanoparticles. The elemental analysis was performed by energy-dispersive-ray spectroscopy (EDS or EDX). The EDS spectrum confirms the presence of Copper (Cu), Sulfur (S), and traces of Carbon (C) and Oxygen (O) in the sample.

4.0 Conclusion

- Copper Sulfide (CuS) nanoparticles, characterized by a consistent petal-like morphological structure, were synthesized through the hydrothermal method at varying temperatures. The impact of the reaction temperature on nucleation and growth processes is evident, resulting in the development of CuS nanoneedle-like structures that aggregate to form flower-like structures at elevated temperatures. X-ray Diffraction (XRD) studies reveal a noticeable increase in the average particle size of the synthesized CuS nanoparticles, ranging from 17 nm to 26 nm, with discernible XRD peaks corresponding to the Covellite phase. The elevation in reaction temperature is associated with an increase in particle size and a concurrent decrease in the band gap from 2.0 eV to 1.93 eV. Furthermore, the observed maximum absorption in the visible region (400 to 550 nm) suggests that the synthesized CuS nanocomposites hold promising applications in the field of optoelectronics. Nanoparticle Morphology mentions that CuS nanoparticles exhibit petal-like morphology structures and their shape changes as the reaction temperature varies. This information could be relevant in mining for understanding the natural formations of CuS in different geological conditions.
- XRD Studies reveal the average particle size of the synthesized CuS nanoparticles, ranging from 17 to 26nm. This data can be used to study the properties of CuS nanoparticles in mining processes or to analyze the size distribution of CuS in ore samples.

- Optoelectronic Potential about maximum absorption in the visible region (400 to 550nm) suggests that the synthesized CuS nanocomposites may have potential applications in optoelectronics. This information may be valuable for exploring the use of CuS in mining-related technology, such as sensors or detectors.

In mining, understanding the properties and potential applications of materials like CuS is crucial for optimizing extraction and processing methods. Additionally, the paragraph hints at the role of temperature in altering CuS properties, which can be important for mining operations conducted at varying temperature conditions.

5.0 References

1. Wei M, Qiao Y, Zhao H, Liang J, Li T, Luo Y, *et al*. Electrochemical non-enzymatic glucose sensors: Recent progress and perspectives. Chem Comm. 2020; 56(93):14553-69. https://doi.org/10.1039/D0CC05650B
2. Gautam UK, Mukherjee B. A simple synthesis and characterization of CuS nanocrystals. Bull Mater Sci. 2006; 29:1-5. https://doi.org/10.1007/BF02709345
3. Sinyagin A, Belov A, Kotov N. Monte Carlo simulation of linear aggregate formation from CdTe nanoparticles. Model Simul Mater Sci Eng. 2005; 13(3):389. https://doi.org/10.1088/0965-0393/13/3/008
4. Yepsen O, Yáñez J, Mansilla HD. Photocorrosion of copper sulfides: Toward a solar mining industry. Sol Energy. 2018; 171:106-11. https://doi.org/10.1016/j.solener.2018.06.049
5. Zhang Y, Qiao ZP, Chen XM. Microwave-assisted elemental direct reaction route to nanocrystalline copper chalcogenides CuSe and Cu_2Te. J Mater Chem. 2002; 12(9):2747-8. https://doi.org/10.1039/b205558a
6. Zhao Y, Shao Y, Chen H, Luo X, Liu X. The facile synthesis of hollow CuS microspheres assembled from nanosheets for Li-ion storage and photocatalytic applications. Nanomaterials. 2023; 13(9):1505. https://doi.org/10.3390/nano13091505
7. Nath SK, Kalita PK. Effect of growth condition on the structural, optical and ionic characteristics of chemically synthesized CuS nanostructures in starch matrix. Bulg J Phys. 2023; 50(3). https://doi.org/10.55318/bgjp.2023.50.3.280
8. Ji H, Cao J, Feng J, Chang X, Ma X, Liu J, *et al*. Fabrication of CuS nanocrystals with various morphologies in the presence of a nonionic surfactant. Mater Lett. 2005; 59(24-25):3169-72. https://doi.org/10.1016/j.matlet.2005.05.046
9. Yao C, Chen S, Wang L, Deng H, Tong S. Low cost and rapid fabrication of copper sulfides nanoparticles for selective and efficient capture of noble metal ions. Chem Eng J. 2019; 373:1168-78. https://doi.org/10.1016/j.cej.2019.05.070
10. Roy P, Mondal K, Srivastava SK. Synthesis of twinned CuS nanorods by a simple wet chemical method. Cryst Growth Des. 2008; 8(5):1530-4. https://doi.org/10.1021/cg700780k
11. Pandey RK, Tsai CL, Liu CP. Ex-situ study on the evolution of cubic cu1. 8s nanowires and nanobelts with two-dimensional multivariant superlattices by cation exchange. J Phys Chem C. 2021; 125(27):14590-8. https://doi.org/10.1021/acs.jpcc.1c01520
12. Yang YJ, Xiang JW. Template-free synthesis of CuS nanorods with a simple aqueous reaction at ambient conditions. Appl Phys. A. 2005; 81(7):1351-3. https://doi.org/10.1007/s00339-005-3292-3
13. Wu C, Shi JB, Chen CJ, Chen YC, Lin YT, Wu PF, *et al*. Synthesis and optical properties of CuS nanowires fabricated by electrodeposition with anodic alumina membrane. Mater Lett. 2008; 62(6-7):1074-7. https://doi.org/10.1016/j.matlet.2007.07.046
14. Kushwah R, Singh A, Anshul A, Mishra D, Amritphale SS. Facile and controlled synthesis of copper sulfide nanostructures of varying morphology. J Mater Sci: Mater. Electron. 2016; 28(7):5597–602. https://doi.org/10.1007/s10854-016-6227-1
15. Saranya M, Grace AN. Hydrothermal synthesis of CuS nanostructures with different morphology. J Nano Res. 2012; 18:43-51. https://doi.org/10.4028/www.scientific.net/JNanoR.18-19.43
16. Qin AM, Fang YP, Ou HD, Liu HQ, Su CY. Formation of various morphologies of covellite copper sulfide submicron crystals by a hydrothermal method without surfactant. Cryst Growth Des. 2005; 5(3):855-60. https://doi.org/10.1021/cg049736o
17. Chun Zeng H. Ostwald ripening: A synthetic approach for hollow nanomaterials. Curr Nanosci. 2007; 3(2):177-81. https://doi.org/10.2174/157341307780619279
18. Tetyana P, Mphuthi N, Jijana AN, Moloto N, Shumbula PM, Skepu A, *et al*. Synthesis, characterization, and electrochemical evaluation of copper sulfide nanoparticles and their application for non-enzymatic glucose detection in blood samples. Nanomater. 2023; 13(3):481. https://doi.org/10.3390/nano13030481
19. Suriakarthick R, Kumar VN, Indirajith R, Shyju TS, Gopalakrishnan R. Photochemically deposited and post annealed copper indium disulphide thin films. Superlattices Microstruct. 2014; 75:667-79. https://doi.org/10.1016/j.spmi.2014.08.012
20. Chen L, Yu W, Li Y. Synthesis and characterization of tubular CuS with flower-like wall from a low temperature hydrothermal route. Powder Technol. 2009; 191(1-2):52-4. https://doi.org/10.1016/j.powtec.2008.09.007
21. Xu H, Wang W, Zhu W, Zhou L. Synthesis of octahedral CuS nanocages via a solid-liquid reaction. Nanotech. 2006; 17(15):3649. https://doi.org/10.1088/0957-4484/17/15/005

22. Jiang J, Jiang Q, Deng R, Xie X, Meng J. Controllable preparation, formation mechanism and photocatalytic performance of copper base sulfide nanoparticles. Mater Chem Phys. 2020; 254:123504. https://doi.org/10.1016/j.matchemphys.2020.123504
23. Rehman S, Mumtaz A, Hasanain SK. Size effects on the magnetic and optical properties of CuO nanoparticles. J Nanoparticle Res. 2011; 13:2497-507. https://doi.org/10.1007/s11051-010-0143-8
24. Kore RH, Kulkarni JS, Haram SK. Effect of nonionic surfactants on the kinetics of disproportion of copper sulfide nanoparticles in the aqueous sols. Chem Mater. 2001; 13(5):1789-93. https://doi.org/10.1021/cm010013r
25. Yang C, Fan H, Xi Y, Chen J, Li Z. Effects of depositing temperatures on structure and optical properties of TiO2 film deposited by ion beam assisted electron beam evaporation. Appl Surf Sci. 2008; 254(9):2685-9. https://doi.org/10.1016/j.apsusc.2007.10.006
26. Silvester EJ, Grieser F, Sexton BA, Healy TW. Spectroscopic studies on copper sulfide sols. Langmuir. 1991; 7(12):2917-22. https://doi.org/10.1021/la00060a009
27. Ramamoorthy C, Rajendran V. Synthesis and characterization of CuS nanostructures: Structural, optical, electrochemical and photocatalytic activity by the hydro/solvothermal process. Int J Hydrogen Energy. 2017; 42(42):26454-63. https://doi.org/10.1016/j.ijhydene.2017.07.078
28. Bhargava RN, Haranath D, Mehta A. Bandgap engineering and doping of ZnO and ZnOS nanocrystals. J Korean Phys Soc. 2008; 53(9):2847-51. https://doi.org/10.3938/jkps.53.2847
29. Iqbal S, Shaid NA, Sajid MM, Javed Y, Fakhar-e-Alam M, Mahmood A, *et al*. Extensive evaluation of changes in structural, chemical and thermal properties of copper sulfide nanoparticles at different calcination temperature. J Cryst Growth. 2020; 547:125823. https://doi.org/10.1016/j.jcrysgro.2020.125823
30. Muddassir Y, Tahir S, Ali A, Mahmood K, Ur Rehman U, Ashfaq A, *et al*. Morphology-dependent thermoelectric properties of mixed phases of copper sulfide (Cu_2– x S) nanostructures synthesized by hydrothermal method. Appl Phys. A. 2021; 127(6):457. https://doi.org/10.1007/s00339-021-04599-2
31. Kushwah R, Singh A, Anshul A, Mishra D, Amritphale SS. Facile and controlled synthesis of copper sulfide nanostructures of varying morphology. J Mater Sci: Mater Electron. 2017; 28:5597-602. https://doi.org/10.1007/s10854-016-6227-1